Combustion and Flame 252 (2023) 112753

Contents lists available at ScienceDirect

Combustion and Flame

journal homepage: www.elsevier.com/locate/combustflame

Brief Communications

Reaction mechanisms of alkyloxiranes for combustion modeling

Nicholas S. Dewey[a], Brandon Rotavera[a,b,*]

[a] Department of Chemistry, University of Georgia, Athens, GA 30602, United States
[b] College of Engineering, University of Georgia, Athens, GA 30602, United States

ARTICLE INFO

Article history:
Received 18 December 2022
Revised 20 March 2023
Accepted 22 March 2023

Keywords:
Mechanism truncation error
QOOH
Low-temperature combustion
RMG
Automated mechanism generation
Cyclic ethers

ABSTRACT

Cyclic ethers are intermediates formed from unimolecular reaction of carbon-centered hydroperoxy-substituted radicals (ȮOOH), which are central to low-temperature chain-branching. Because cyclic ethers are isomer-specific proxies for ȮOOH, detailed prescription of chemical reactions describing the consumption mechanisms is required for accurate combustion modeling. However, the most common approach in the development of chemical kinetics mechanisms is to use a simplified set of elementary steps that neglect the formation and subsequent reaction of cyclic ether radicals, which creates a source of mechanism truncation error. As a consequence, quantitative discrepancies between model predictions and experimental species profiles of cyclic ethers are ubiquitous and span a range of hydrocarbons such as *n*-butane, *n*-pentane, *n*-hexane, cyclohexane, hexene isomers, and hexanal. Moreover, uncertainties in species profile predictions of cyclic ethers translate directly to uncertainty in ignition predictions.

For the explicit purpose of determining the extent to which cyclic ether consumption mechanisms affect combustion modeling, the present work examines the chemical kinetics underpinning such discrepancies using, as a representative case, a subset of cyclic ethers produced from *n*-butane oxidation. Detailed sub-mechanisms are developed using Reaction Mechanism Generator (RMG) for ethyloxirane and 2,3-dimethyloxirane, which form from unimolecular decomposition of β-ȮOOH radicals during *n*-butane combustion. The sub-mechanisms prescribe consumption reactions for both cyclic ethers, including ȮH-initiated H-abstraction, O_2-addition, ROȮ isomerization, among other reactions, and were integrated with the NUIGMech1.1 mechanism to examine model predictions of species profiles and ignition delay times.

Inclusion of the sub-mechanisms led to closer consistency between model predictions and experimental species profiles and also affected ignition predictions. Sensitivity analysis shows that rates of ȮH-initiated H-abstraction are critical for determining temperature dependence of species profiles of cyclic ethers, which may serve as an indicator for the importance of branching fractions in the initiation step ȮH + *n*-butane → H_2O + 1–butyl/2–butyl. Moreover, flux towards ketohydroperoxide formation from *n*-butane increased upon addition of the sub-mechanisms, as determined by rate-of-production analyses conducted on ȮH and related impact on ignition delay time simulations.

The results herein demonstrate that detailed sub-mechanisms and accurate H-abstraction rates from cyclic ethers are necessary for high-fidelity predictions of chemical kinetics for combustion modeling. Continued refinement of detailed reaction mechanisms is required in order to produce accurate models for combustion that serve as a starting point for mechanism reduction techniques applied either to detailed mechanisms or to sub-mechanisms for consequent integration. Such techniques are required to enable modeling of reactive flows that incorporate computational fluid dynamics at practical conditions.

1. Introduction

For low-temperature combustion modeling, detailed chemical kinetics mechanisms must include reactions involving carbon-centered hydroperoxy-substituted radicals (ȮOOH) because such species generate radicals that control ignition behavior [1]. Given the abundance of isomers and complex potential energy surfaces, mechanisms often contain thousands of species and reactions. Significant advances in automated mechanism development [2,3] with programs such as Reaction Mechanism Generator (RMG), which generates chemical kinetics mechanisms using a flux-based model-expanding algorithm [4,5], enables the expansion of reaction networks to include such complexities.

Two competitive pathways consume ȮOOH in the forward direction: bimolecular reaction with O_2 and unimolecular decomposition [1,6]. The latter yields cyclic ether intermediates formed coincident with ȮH in a chain-propagating step (**S1**) and are direct,

* Corresponding author.
E-mail address: rotavera@uga.edu (B. Rotavera).

https://doi.org/10.1016/j.combustflame.2023.112753
0010-2180/

isomer-specific proxies for reactions of ȮOOH, yet are measured in limited cases [7–9]. In addition to direct contributions to ȮH populations, cyclic ethers can also yield products attributed to other classes of molecules [10]. One notable example is dicarbonyls [10–12], which are considered to form via ketohydroperoxides [13]. To minimize mechanism truncation error – uncertainty derived from incomplete sub-mechanisms – chemical kinetics mechanisms must accurately predict species profiles of cyclic ethers [6,14], which remains a ubiquitous issue for alkanes, alkenes, and aldehydes (**S2**).

As one example, speciation experiments show that cyclic ether formation corresponding to the negative temperature coefficient behavior of *n*-butane yields concentration peaks at 650 K and 800 K – a gap of ∼150 K [15]. However, species profiles predicted by chemical kinetics mechanisms, such as for ethyloxirane and 2,3-dimethyloxirane, which are two cyclic ethers formed in abundance from β-ȮOOH during *n*-butane combustion [11,12,16,17], exhibit a narrower gap of ∼120 K between concentration peaks [13,18–21]. Such discrepancies may arise from uncertainty in cyclic ether chemistry, which Hartness et al. [15] show to cause significant shifts in ignition delay time predictions of *n*-butane. For example, current chemical kinetic mechanisms of *n*-butane truncate cyclic ether consumption reactions in which, at most, two consumption reactions are prescribed for ethyloxirane and 2,3-dimethyloxirane [13,18–21]. The placeholder reactions neglect H-abstraction reactions that form distinct radicals and subsequent reaction via unimolecular decomposition or O_2-addition [11,12].

The objective of the present work is not to propose a revised *n*-butane mechanism. Rather, drawing upon the complexities of cyclic ethers [10–12], detailed analysis is carried out to examine the extent to which sub-mechanisms developed for ethyloxirane and 2,3-dimethyloxirane impact *n*-butane combustion modeling targets. Modeling of species profiles is conducted to examine the aforementioned discrepancies for the first time by integrating the sub-mechanisms that prescribe detailed consumption chemistry into NUIGMech1.1 and juxtaposing uncertainty in cyclic ether profiles with uncertainty in ignition predictions.

2. Methodology

Detailed sub-mechanisms for ethyloxirane and 2,3-dimethyloxirane were constructed using RMG v3.1 [4,5], guided by speciation measurements and potential energy surfaces in Doner et al. [11] and Christianson et al. [12]. In total, 884 new species and 3828 reactions were added to NUIGMech1.1 [20]. RMG produced reactions from numerous classes of oxidation and unimolecular decomposition reactions of both cyclic ethers (**S3**) that are typical in low-temperature combustion, including all possible ROȮ radicals. Figure S3.1 shows reaction pathways for ethyloxirane and 2,3-dimethyloxirane around which the sub-mechanisms were developed. Stereoisomers of 2,3-dimethyloxirane [11] were not considered separately because RMG neglects stereochemistry and, consequently, stereochemical-dependent reactions.

Rates of elementary reactions were produced by RMG using rate rules [22] and thermodynamic properties were calculated via Benson group additivity methods [23]. The number of oxygen atoms for all species in the sub-mechanisms was restricted to three, meaning that second O_2-addition to ȮOOH derived from cyclic ethers was neglected based on the experiments of Doner et al. [11] and Christianson et al. [12] in which products only from unimolecular reactions of Ṙ and ȮOOH, not from ȮOOH + O_2, were detected. Additional detail pertaining to the construction of the sub-mechanisms, including reactor conditions, model tolerances, and RMG input files are in S4.

To examine the efficacy of rate rules, RMG-generated rate parameters of ȮH-initiated H-abstraction from ethyloxirane and 2,3-dimethyloxirane were replaced with parameters from analogous reactions of 2-butyltetrahydrofuran [24] and 2,5-dimethyltetrahydrofuran [25], respectively. C–H bonds on carbons α, α', and β to the oxygen atom in 2-butyltetrahydrofuran, as well as on the primary carbon of the *n*–butyl group, were selected as H-abstraction sites for comparison with ethyloxirane. Similarly, for 2,5-dimethyltetrahydrofuran, C–H bonds on the carbon α to the oxygen atom and β on the methyl group were selected for comparison with 2,3-dimethyloxirane.

Simulations using NUIGMech1.1 and the modifications (Table S4.1) were conducted using the PSR model in ChemKin 19.2 with fixed gas temperature and steady-state solver settings. Sensitivity and rate-of-production analyses were also conducted. An initial *n*-butane mole fraction of 0.02 under stoichiometric conditions, pressure of 1.1 atm, and residence time of 4.0 s were employed for modeling species profiles from 500 K to 1000 K, consistent with the conditions from Hartness et al. [15]. Ignition simulations were performed at constant pressure (10 atm) in the closed homogenous reactor model (S5) to isolate the chemical influence of the cyclic ether sub-mechanisms.

3. Results and discussion

The measured local maxima in the yield of 2,3-dimethyloxirane stereoisomers occur at 650 K and 800 K [15], a gap of 150 K (Fig. 1a), while the NUIGMech1.1 predictions indicate a narrower gap of ∼120 K. By accounting for consumption reactions and replacing the placeholder reactions in NUIGMech1.1 with the sub-mechanisms herein, the model predictions became more consistent with the experimental trends: the gap between predicted local maxima increased to 160 K for 2,3-dimethyloxirane. Similar effects occurred for ethyloxirane (S5). The results in Figs. 1a and S5a show that the initial addition of consumption reactions in the sub-mechanisms led to an increase in the concentration of both cyclic ethers despite the rate coefficient for ȮOOH → cyclic ether + ȮH being unaltered. The increase in predicted concentrations using the first modification is likely due to a decrease in the total consumption rate of ethyloxirane and 2,3-dimethyloxirane, as shown in a comparison between the rates prescribed in NUIGMech1.1 to the rates of H-abstraction in the expanded sub-mechanism developed herein (**S6**).

Sensitivity analyses were conducted at both local maxima of ethyloxirane and 2,3-dimethyloxirane (**S7**) and show that H-abstraction reactions significantly affect species profiles of both cyclic ethers. As a result, RMG-generated H-abstraction rates were replaced with ones from analogous reactions to produce the second modification (cf. Table S4.1). Only ȮH-initiated H-abstractions were considered because ȮH is the dominant abstractor for both species, as indicated by rate-of-production analysis (S8). The impact of replacing H-abstraction rates (S9) on the species profiles of 2,3-dimethyloxirane isomers is shown in Fig. 1a. The shape of the species profile matches that from NUIGMech1.1. However, the predicted concentrations for 2,3-dimethyloxirane decreased at both local maxima by an average of 55% compared to the first modified mechanism, bringing the model into closer consistency with the experiments. Similar effects were shown for ethyloxirane (**S5**). The results demonstrate that ȮH-initiated H-abstraction reactions significantly influence species profiles of ethyloxirane and 2,3-dimethyloxirane. Sensitivity analyses were subsequently conducted on the mechanism after the second modification to analyze the reason for the observed changes in species profiles (**S7**) and reaffirmed that rates of ȮH-initiated H-abstraction from cyclic ethers impact predictions of temperature dependence.

Significant effects on ignition delay time predictions below 800 K for *n*-butane (Fig. 1b) also resulted from integration of the sub-mechanisms for ethyloxirane and 2,3-dimethyloxirane, and provide insight on the implications of incorporating detailed consump-

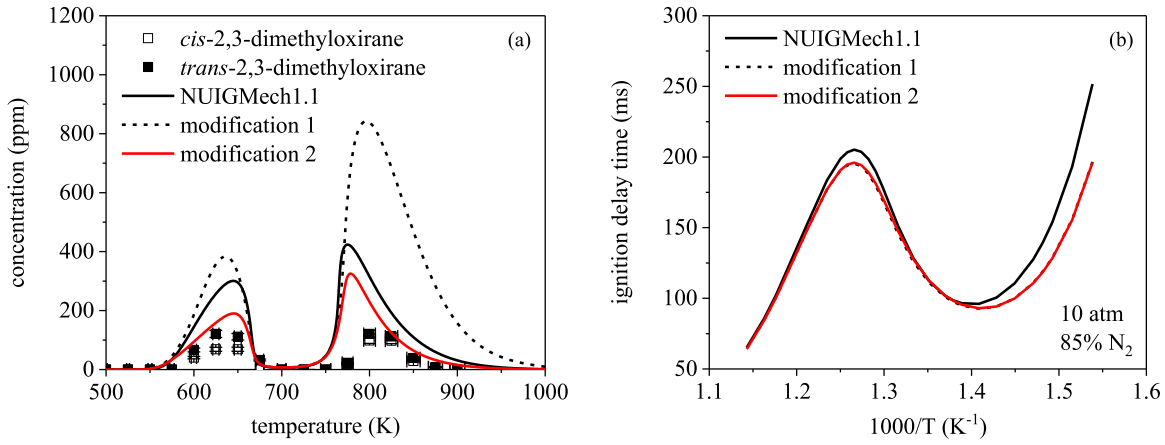

Fig. 1. (a) Species profiles of *cis*- and *trans*- stereoisomers of 2,3-dimethyloxirane [15]; model predictions neglect stereoisomers. (b) Stoichiometric ignition delay time simulations of *n*-butane. Accounting for complete description of cyclic ether reactions improves species profile predictions and affects the prediction of ignition delay times for *n*-butane due to direct connection to ȮOOH and chain-branching behavior. The sensitivity of model predictions to cyclic ether reactions underscores the impact of mechanism truncation error.

tion reactions of cyclic ethers into chemical kinetics mechanisms. Adding such pathways affirms that products of cyclic ether consumption influence the chain-reaction sequence leading to ignition due partly to involvement in the formation of other intermediates produced during *n*-butane combustion. For example, ring-opening of alkyloxiranes can form resonance-stabilized ketohydroperoxide-type radicals [11,12], which are also produced via H-abstraction of ketohydroperoxides, as an alternative to chain-branching (S10). The resonance-stabilized radicals can react with O_2 to yield the same species that may otherwise form from third-O_2 addition of the parent hydrocarbon. The comparison in Fig. 1 indicates that including all production and consumption pathways in chemical kinetics mechanisms for cyclic ethers of *n*-butane, as well as for other hydrocarbon and biofuels, is critical for producing high-fidelity combustion models.

Declaration of Competing Interest

None.

Acknowledgments

BR acknowledges support by the National Science Foundation (NSF) under Grant No. 2042646 and Grant No. 2125064. N.S.D. was supported in part by the U.S. Department of Transportation, Federal Highway Administration, Talent Development Division, Dwight David Eisenhower Transportation Fellowship Program Graduate Fellowship under Grant No. 693JJ32245090.

Supplementary materials

Supplementary material: doi:10.1016/j.combustflame.2023.112753.

References

[1] J. Zádor, C.A. Taatjes, R.X. Fernandes, Kinetics of elementary reactions in low-temperature autoignition chemistry, Prog. Energy Combust. Sci. 37 (2011) 371–421.
[2] S.N. Elliott, K.B. Moore III, A.V. Copan, M. Keceli, C. Cavallotti, Y. Georgievskii, H.F. Schaefer III, S.J. Klippenstein, Automated theoretical chemical kinetics: predicting the kinetics for the initial stages of pyrolysis, Proc. Combust. Inst. 38 (2021) 375–384.
[3] J.A. Miller, R. Sivaramakrishnan, Y. Tao, C.F. Goldsmith, M.P. Burke, A.W. Jasper, N. Hansen, N.J. Labbe, P. Glarborg, J. Zádor, Combustion chemistry in the twenty-first century: developing theory-informed chemical kinetics models, Prog. Energy Combust. Sci. 83 (2021) 100886.
[4] C.W. Gao, J.W. Allen, W.H. Green, R.H. West, Reaction mechanism generator: automatic construction of chemical kinetic mechanisms, Comput. Phys. Commun. 203 (2016) 212–225.
[5] M. Liu, A. Grinberg Dana, M.S. Johnson, M.J. Goldman, A. Jocher, A.M. Payne, C.A. Grambow, K. Han, N.W. Yee, E.J. Mazeau, Reaction mechanism generator v3.0: advances in automatic mechanism generation, J. Chem. Inf. Model. 61 (2021) 2686–2696.
[6] B. Rotavera, C.A. Taatjes, Influence of functional groups on low-temperature combustion chemistry of biofuels, Prog. Energy Combust. Sci. 86 (2021) 100925.
[7] J. Zádor, H. Huang, O. Welz, J. Zetterberg, D.L. Osborn, C.A. Taatjes, Directly measuring reaction kinetics of QOOH–a crucial but elusive intermediate in hydrocarbon autoignition, Phys. Chem. Chem. Phys. 15 (2013) 10753–10760.
[8] J.D. Savee, E. Papajak, B. Rotavera, H. Huang, A.J. Eskola, O. Welz, L. Sheps, C.A. Taatjes, J. Zádor, D.L. Osborn, Direct observation and kinetics of a hydroperoxyalkyl radical (QOOH), Science 347 (2015) 643–646.
[9] A.S. Hansen, T. Bhagde, K.B. Moore III, D.R. Moberg, A.W. Jasper, Y. Georgievskii, M.F. Vansco, S.J. Klippenstein, M.I. Lester, Watching a hydroperoxyalkyl radical (•QOOH) dissociate, Science 373 (2021) 679–682.
[10] A.C. Doner, J. Zádor, B. Rotavera, Stereoisomer-dependent unimolecular kinetics of 2,4-dimethyloxetanyl peroxy radicals, Faraday Discuss. 238 (2022) 295–319.
[11] A.C. Doner, M.M. Davis, A.L. Koritzke, M.G. Christianson, J.M. Turney, H.F. Schaefer III, L. Sheps, D.L. Osborn, C.A. Taatjes, B. Rotavera, Isomer-dependent reaction mechanisms of cyclic ether intermediates: cis-2,3-dimethyloxirane and trans-2,3-dimethyloxirane, Int. J. Chem. Kinet. 53 (2021) 127–145.
[12] M.G. Christianson, A.C. Doner, M.M. Davis, A.L. Koritzke, J.M. Turney, H.F. Schaefer III, L. Sheps, D.L. Osborn, C.A. Taatjes, B. Rotavera, Reaction mechanisms of a cyclic ether intermediate: ethyloxirane, Int. J. Chem. Kinet. 53 (2021) 43–59.
[13] F. Battin-Leclerc, O. Herbinet, P.A. Glaude, R. Fournet, Z. Zhou, L. Deng, H. Guo, M. Xie, F. Qi, New experimental evidences about the formation and consumption of ketohydroperoxides, Proc. Combust. Inst. 33 (2011) 325–331.
[14] L.-S. Tran, O. Herbinet, H.H. Carstensen, F. Battin-Leclerc, Chemical kinetics of cyclic ethers in combustion, Prog. Energy Combust. Sci. 92 (2022) 101019.
[15] S.W. Hartness, N.S. Dewey, M.G. Christianson, A.L. Koritzke, A.C. Doner, A.R. Webb, B. Rotavera, Probing O_2 dependence of hydroperoxy-butyl reactions via isomer-resolved speciation, Proc. Combust. Inst. 39 (2023).
[16] O. Herbinet, F. Battin-Leclerc, S. Bax, H. Le Gall, P.A. Glaude, R. Fournet, Z. Zhou, L. Deng, H. Guo, M. Xie, Detailed product analysis during the low temperature oxidation of n-butane, Phys. Chem. Chem. Phys. 13 (2011) 296–308.
[17] A.J. Eskola, O. Welz, J.D. Savee, D.L. Osborn, C.A. Taatjes, Synchrotron photoionization mass spectrometry measurements of product formation in low-temperature n-butane oxidation: toward a fundamental understanding of autoignition chemistry and n-C_4H_9+ O_2/s-C_4H_9+ O_2 reactions, J. Phys. Chem. A 117 (2013) 12216–12235.
[18] D. Healy, N. Donato, C. Aul, E. Petersen, C. Zinner, G. Bourque, H. Curran, n-Butane: ignition delay measurements at high pressure and detailed chemical kinetic simulations, Combust Flame 157 (2010) 1526–1539.
[19] M. Cord, B. Sirjean, R. Fournet, A. Tomlin, M. Ruiz-Lopez, F. Battin-Leclerc, Improvement of the modeling of the low-temperature oxidation of n-butane: study of the primary reactions, J. Phys. Chem. A 116 (2012) 6142–6158.
[20] A.A.E.-S. Mohamed, S. Panigrahy, A.B. Sahu, G. Bourque, H.J. Curran, An experimental and kinetic modeling study of the auto-ignition of natural gas blends containing C1–C7 alkanes, Proc. Combust. Inst. 38 (2021) 365–373.
[21] Y. Wu, S. Panigrahy, A.B. Sahu, C. Bariki, J. Beeckmann, J. Liang, A.A. Mohamed, S. Dong, C. Tang, H. Pitsch, Understanding the antagonistic effect of methanol as a component in surrogate fuel models: a case study of methanol/n-heptane mixtures, Combust. Flame 226 (2021) 229–242.

[22] R.G. Susnow, A.M. Dean, W.H. Green, P. Peczak, L.J. Broadbelt, Rate-based construction of kinetic models for complex systems, J. Phys. Chem. A 101 (1997) 3731–3740.
[23] S.W. Benson, J.H. Buss, Additivity rules for the estimation of molecular properties. thermodynamic properties, J. Chem. Phys. 29 (1958) 546–572.
[24] L. Cai, H. Minwegen, J. Beeckmann, U. Burke, R. Tripathi, A. Ramalingam, L.C. Kröger, A. Sudholt, K. Leonhard, J. Klankermayer, Experimental and numerical study of a novel biofuel: 2-butyltetrahydrofuran, Combust. Flame 178 (2017) 257–267.
[25] Y. Fenard, H. Song, H. Minwegen, P. Parab, C.S. Mergulhão, G. Vanhove, K.A. Heufer, 2,5-dimethyltetrahydrofuran combustion: ignition delay times at high and low temperatures, speciation measurements and detailed kinetic modeling, Combust. Flame 203 (2019) 341–351.